The International Journal of Advanced Manufacturing Technology (2018) 97:2767–2779
https://doi.org/10.1007/s00170-018-2147-y

ORIGINAL ARTICLE

Effect of process parameters on mechanical properties of friction stir welded dissimilar 7075-T651 and 5083-H111 aluminum alloys

Izabela Kalemba-Rec[1] · Mateusz Kopyściański[1] · Damian Miara[2] · Krzysztof Krasnowski[2]

Received: 5 January 2018 / Accepted: 7 May 2018 / Published online: 21 May 2018

Abstract
In this paper, the influence of process parameters (tool rotational speed, pin design, and configuration of joined alloys) on the macrostructure and mechanical properties of friction stir welded aluminum alloys 7075-T651 and 5083-H111 was characterized. The tool rotational speed and the alloy placement significantly influenced the formation of the weld (especially the stir zone). Superior mixing of materials was obtained at higher rotational speeds and in the configuration with 5083 on the advancing side and 7075 on the retreating side. However, under these conditions, more defects, such as porosity, voids, or wormholes, were found in the stir zone. Regardless of the pin design and weld configuration, with an increasing tool rotational speed, the mechanical properties decrease. Using the Triflute pin, however, guarantees higher tensile strength and weld efficiency (above 100%). The weld configuration did not influence the mechanical properties. The highest tensile strength (371 MPa) defect-free joint was obtained with 5083 on the advancing side, 7075 on the retreating side, a tool rotational speed of 280 rpm, and the Triflute pin.

Keywords Dissimilar alloys joining · Friction stir welding · Process parameters · Mechanical properties · Microstructure

1 Introduction

The simplicity of friction stir welding (FSW) technology (Fig. 1a) and the absence of melting suggest the application of this process to the joining of dissimilar aluminum alloys and obtaining defect-free welds with good mechanical properties. However, before FSW can be fully and broadly implemented in industry, especially for dissimilar materials, optimization of the process parameters is required. During the process, numerous parameters influence the heat generation and material mixing and determine the weld's final quality and properties [1, 2]. The two principal parameters are tool rotational speed and welding speed (often referred to as the traverse speed); however, tool shape and its dimensions (i.e., pin diameter, pin length, shoulder diameter, shoulder concavity angle), tool tilt angle, plunge depth, vertical force, thickness of welded plates, weld configuration, alloy composition, and its initial temper also play a substantial role [3–5]. Therefore, many investigations have focused on the parameters of the FSW process and their effect on properties and microstructure of welds. Influence of tool rotational speed [6–9], welding speed [7–11], configuration of welded alloys [10, 12], and pin geometry [6, 13–15] on welding of dissimilar aluminum alloys has been extensively examined to date.

In this research, the effect of three different factors, tool rotational speed, pin design, and configuration of joined alloys (alloy placement on the advancing or retreating side), on the macrostructure and mechanical properties of dissimilar friction stir welds was examined. The investigation presented here characterizes welds between 7075-T651 and 5083-H111 commercial aluminum alloys. 5083 is suitable for all standard electric and resistance methods of welding, but 7075, due to the presence of copper, exhibits poor weldability by conventional fusion joining processes. Thus, the application of FSW seems to be an adequate technique to obtain good quality welds. Several published papers have already reported studies on friction stir welding of 5xxx and 7xxx series Al alloys [7, 8, 16–20]. Ahmed et al. [19] discussed the influence

✉ Izabela Kalemba-Rec
kalemba@agh.edu.pl

[1] Faculty of Metal Engineering and Industrial Computer Science, AGH University of Science and Technology, Av. Mickiewicza 30, 30-059 Kraków, Poland

[2] Instytut Spawalnictwa (Institute of Welding), 16-18 Bł. Czesława Str., 44-100 Gliwice, Poland

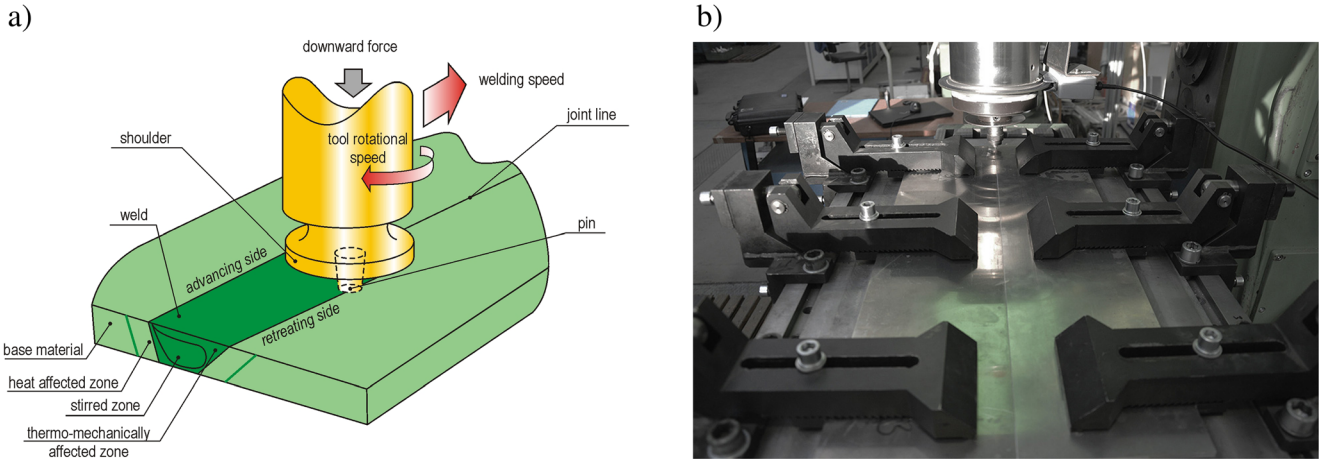

Fig. 1 Friction stir welding. **a** A scheme of the process. **b** An experimental setup with the clamping system

of the welding speed on microstructure, hardness, and tensile properties of dissimilar welds between 5083-H111 and 7075-T6 alloys (with 5083 alloy on the advancing side). However, their results showed that an increase in the welding speed does not have a significant effect on grain size, hardness, or tensile strength. The ultimate tensile strengths of joints ranged between 245 and 267 MPa. In another work, Ahmed et al. [17] investigated friction stir welded joints between 7075-T6 and 5052-H34 alloys with 7075 located on the advancing side. The maximum tensile strength of these joints approached 198 MPa. The friction stir welds between 5083 (on the advancing side) and 7075 Al alloys were also examined by Saedi et al. [18]. They attempted to predict optimum conditions for friction stir welding of these alloys using experimental and numerical methods. The highest tensile strength (above 290 MPa) defect-free weld was obtained at a welding speed of 50 mm/min and rotational speeds of 500 and 800 rpm. Shojaeefard et al. [16] in their research focused on microstructure and mechanical properties of friction stir welded 7075-O and 5083-O alloys with 7075 on the advancing side and 5083 on the retreating side. The researchers also optimized the FSW process using a neural network and particle swarm algorithm. The joint produced at a tool rotational speed of 1400 rpm and a welding speed of 20 mm/min was characterized by the highest strength (267 MPa). S. Kasman and Z. Yenier [7] reported investigations of dissimilar FSW welds between 5754-H111 and 7075-T651 alloys (5754 alloy placed on the retreating side). They analyzed the relationships between process parameters (tool diameter, tool rotational speed, and welding speed), microstructure, and mechanical properties of joints. The highest ultimate tensile strength (239 MPa) defect-free weld was achieved with a tool diameter of 22 mm, a tool rotational speed of 1000 rpm, and a welding speed of 80 mm/min. Sivachidambaram et al. [8] produced friction stir welds between 5383 and 7075 alloys using different tool rotational and welding speeds. Here, 7075 was placed on the advancing side. A maximum tensile strength of 211 MPa was obtained for a tool rotational speed of 700 rpm and a welding speed of 40 mm/min. Chen et al. [20] characterized the microstructure and mechanical properties of 5083–7B04 welds. In this study, three variants of heat treatment, artificial aging, natural aging, and annealing, were adopted for the 7B04 alloy. The best material mixing and mechanical properties (tensile strength of 525 MPa) were obtained for the joint between the 5083 alloy (placed on the advancing side) and the artificially aged 7B04 alloy.

While there have been research published in the literature showing that 5xxx and 7xxx alloys can be successfully joined by FSW technology, there is not a complete knowledge of the effect of process parameters on properties of these joints. The final properties of welds are dependent on many interrelated factors, and as such, the influence of a particular parameter is difficult to assess. Hence, the present study aims to provide further insight into the proper selection of process parameters (i.e., tool rotational speed, pin design, and alloy location) that guarantees sound joints between 7075 and 5083 alloys with adequate mechanical properties.

2 Experimental

2.1 Friction stir welding

Dissimilar aluminum alloy sheets of 7075-T651 and 5083-H111 were friction stir welded at the Instytut Spawalnictwa (Welding Institute) in Gliwice, Poland. The FSW setup with clamping system is shown in Fig. 1b. The concentration of main alloying elements (determined by the Perkin Elmer OPTIMA *7300 DV ICP* Optical Emission Spectrometer) and mechanical properties (determined by Wolpert-Wilson Tukon 2500 Vickers hardness tester and MTS 810 tensile testing machine) of base alloys are presented in Tables 1 and 2, respectively.

Table 1 Content of main alloying additions (wt%) and mechanical properties of 7075 Al alloy

Zn	Mg	Cu	Cr	Fe	Tensile stress (MPa)	0.2% yield stress (MPa)	Elongation (%)	Hardness (HV1)
6.18	2.56	1.86	0.21	0.15	604	584	14	180

The thickness of both aluminum alloy plates was 6 mm. The alloys were joined in two butt configurations: one with the 7075 alloy situated on the advancing side (AS) and the 5083 alloy on the retreating side (RS) and the other with the alloy positions reversed. Two different types of tool (Fig. 2) were used for welding. Both tools consisted of a spiral shoulder, but a different pin design: Triflute (developed by TWI) or tapered with a thread. The dimensions of the individual elements of both tools were similar. The details of the tool designs are collected in Table 3.

Experiments were carried out at a constant welding speed of 140 mm/min and a varying tool rotational speed (280, 355, 450, and 560 rpm). The application of lower (140 rpm) or higher (900 rpm) tool rotational speed resulted in the fracture damage of the tool. The downward force was constant and amounted to 26.4 kN.

2.2 Methodology

The photographs of the macrostructure and top surface of the tested welds were obtained with an Olympus SZX7 Stereo Microscope. Macrostructural characterization was supplemented by microstructural examination of the weld center using polarized light microscopy (Zeiss Axio Imager) and EDS (*energy dispersive spectroscopy*) analysis (SEM Inspect S50 with EDAX detector). Cross-sectional metallographic samples were anodizing in a 1.8-ml HBF_4 with 100-ml H_2O electrolyte solution for 40–80 s at room temperature. The current density was 0.2 A/cm^2. The EDS maps were carried out with an acceleration voltage of 15 kV, at working distance of 10 mm. The mechanical properties of all welds were determined by Vickers hardness measurements and tensile tests. The hardness measurements were performed with a Wolpert-Wilson Tukon 2500 hardness tester on the weld cross-section along a line at the mid-plane thickness (i.e., 3 mm from weld surface). The applied load was 1 kg, the indentation time 10 s, and the distance between test points 1 mm. Tensile tests were performed in accordance with ASTM E 8 using an MTS 810 testing machine. The crosshead speed used in the tensile tests was 5 mm/min. Tensile samples were excised perpendicular to the welds in such a way that the weld was centered along the tensile specimen in the reduced section (Fig. 3). A scanning electron microscope Inspect S50 was used for the evaluation of fracture surfaces from ruptured tensile specimens.

3 Results

3.1 Macrostructure

Figure 4 presents macrographs of cross-sections and top surfaces of welds produced with the Triflute pin. Macroscopic observation reveals differences in the macrostructure depending on welding parameters and the alloy configuration and also shows defects in certain welds. The AS 7075–RS 5083 weld produced at 280 rpm is characterized by a distinct boundary between the alloys without any mixing of the materials. Other welds in this configuration and all AS 5083–RS 7075 welds show mixing of the alloys in the weld center. The higher the tool rotational speed, the better the mixing of materials in the weld area. However, a faster rotational speed leads to the formation of macroscopic defects in the weld area, regardless of the alloy's placement. The defects appear at 450 rpm and higher. In the AS 7075–RS 5083 joint produced at 355 rpm, microdefects were observed at higher magnifications in the lower part of the weld area. Porosity, voids, or wormholes occurred most frequently, especially at high tool rotational speeds, in the AS 7075–RS 5083 weld configuration. The defects were located in the stir zone on the advancing side. The advancing side temperatures are hotter than those on the retreating side [21], and at higher tool rotational speeds on the advancing, the excess heat input may be generated resulting in abnormal material stirring and formation of defects. Analysis of the macrostructure suggests that the shape of the region where the material is stirred, observed on the cross-section, changes with an increase in the tool rotational speed. For the lower applied tool rotational speeds, the stirred zone is wide in upper part and narrower in bottom part (takes conical shape). A faster rotation produced a distinct boundary on the

Table 2 Content of main alloying additions (wt%) and mechanical properties of 5083 Al alloy

Mg	Mn	Fe	Si	Tensile stress (MPa)	0.2% yield stress (MPa)	Elongation (%)	Hardness (HV1)
4.32	0.56	0.36	0.16	346	240	23	80

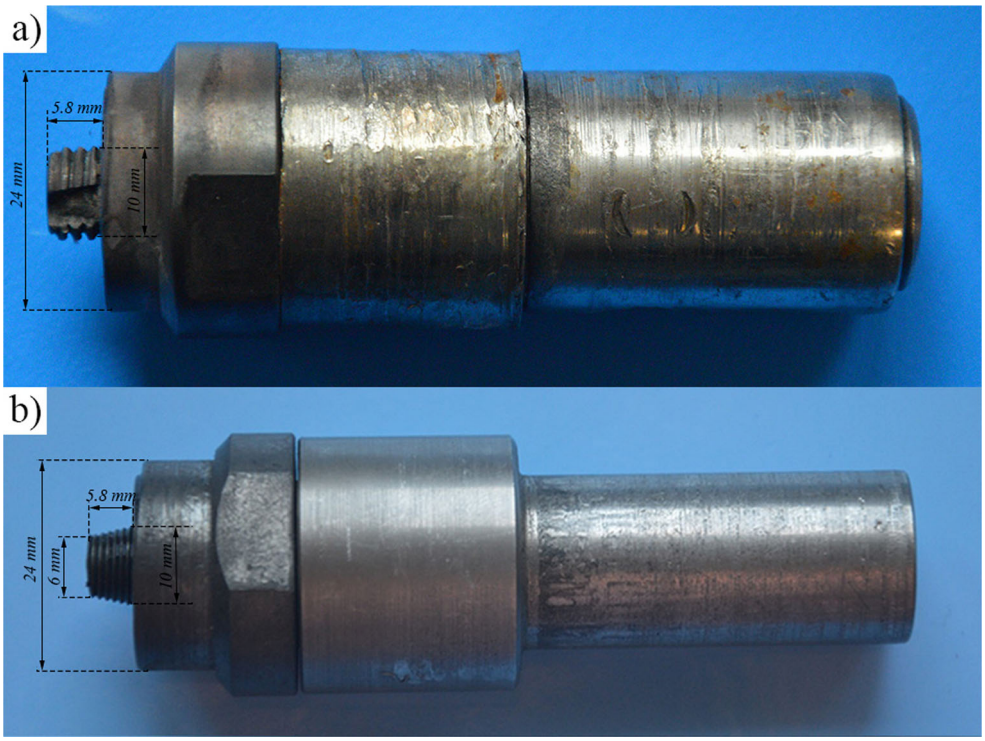

Fig. 2 FSW tool. **a** Triflute pin. **b** Threaded taper pin

advancing side that was oriented perpendicular to the top of the weld surface. The shape of stirred zone becomes more rectangular. In the case of AS 7075–RS 5083, weld delamination and flashes at the surface are observed. A better surface appearance was realized in the opposite configuration. The surface of the AS 5083–RS 7075 welds exhibited clear semicircular features, but at 560 rpm, delamination and ribbon flashes were also observed.

Figure 5 presents the macrostructure of the cross-section and top surface appearance of the welds produced by threaded taper pin. In the welds produced in the AS 7075–RS 5083 configuration, a distinct boundary between the joined alloys was observed. The material intermixing was incomplete; however, the opposite placement of alloys resulted in a better stirring of the material. Regardless of the weld configuration, the tool rotational speed of 560 rpm was too high and led to the creation of voids and wormholes. All defects were located near the top surface on the advancing side (AS 7075–RS 5083 and AS 5083–RS 7075 welds) and at the bottom part of the stir zone (AS 5083–RS 7075 weld). The top surface appearance of all welds exhibited semicircular features with delamination (especially for 560 rpm) and slight ribbon flashes.

Table 3 Details of the used FSW tools

Tools	No. 1	No. 2
Pin feature	Triflute	Threaded taper
Pin diameter	10 mm	10 mm (6 mm on the tip)
Pin length	5.8 mm	5.8 mm
Shoulder diameter	24 mm	24 mm
Shoulder feature	Convex-scrolled	Convex-scrolled
Tool material	HS6-5-2	HS6-5-2

3.2 Microstructure

Light microscopy examinations provided detailed information about the microstructure of the weld center. The weld center of friction stir welds is often referred to as the stirred zone or nugget. This is a region that experiences high temperature and/or severe plastic deformation [3]. Figure 6 shows the microstructure of the center region for selected joints (produced at the lowest and highest rotational speeds, 280 and 560 rpm, respectively). The weld centers for all joints are composed of fine, equiaxed grains that resulted from dynamic recrystallization. It is well established that high temperature and plastic deformation in the stir zone during friction stir welding leads to recrystallization [3, 22]. It was found that for a particular tool rotational speed, no differences in the grain refinement were detected. In other works [7, 16], the influence of the traverse speed, at a constant tool rotational speed, on grain size was described. The size of grains in the stir zone decreased with an increase in the traverse speed, which was attributed to lower heat input. An increase in the tool rotational speed generates a higher heat input and thus a larger grain size is expected. However, in the current study, an increase in the

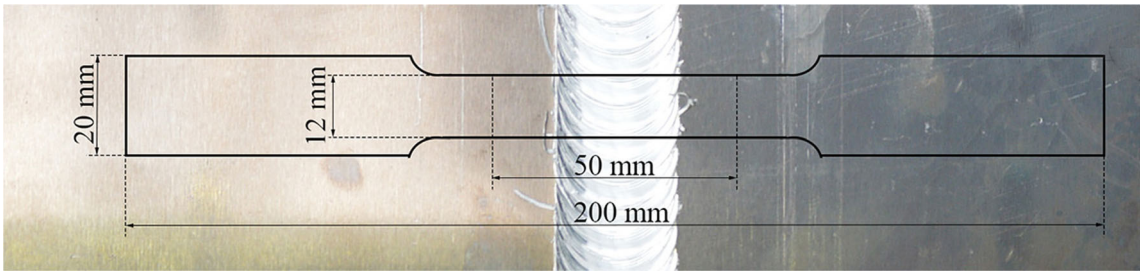

Fig. 3 A scheme showing the manner of excising tensile specimens

grain size was not noticeable; thus, the increase in the heat input was insufficient. Also, Ahmed et al. [19] did not find any difference between grain size with an increase in traverse speed for dissimilar welds between the same alloys as in the current research, i.e., 7075 and 5083. They obtained grain sizes approximately 4 μm at both 50 and 200 mm/min welding speeds.

However, in the current study, the microstructure consisted of regions that differ in grain size. These regions in the form of bands also vary in chemical composition. EDS analysis showed that the particular bands come from both base alloys: one type of band was formed by the 7075 alloy and the other by the 5083 alloy. As shown in Fig. 7, the content of the main constituent elements of the joined alloys (Al-Zn-Mg-Cu and Al-Mg alloys) in the particular bands is different. Depending on the alloy placement, the dominant alloy that occupied the weld center was different. In the AS 7075–RS 5083 welds, the weld center primarily contained magnesium, zinc, and copper. In the case of the AS 5083–RS 7075 configuration, the weld center predominantly contained magnesium with Zn-Mg-Cu bands. Hence, the dominant region of the stir zone mainly includes elements from the alloy located on the advancing side.

3.3 Microhardness

Figure 8 illustrates hardness profiles for welds produced with the Triflute pin in two configurations. In the AS 7075–RS 5083 welds, the profiles for all rotational speeds are very similar; however, for the highest rotational speed (560 rpm), an abrupt hardness drop in the stir zone (3 mm from weld center to advancing side) was observed. The hardness decrease was attributed to the presence of voids in the weld area. In the case of the AS 5083–RS 7075 configuration, the hardness profiles were different. For the lowest applied tool rotational speed (280 rpm), the hardness profile was similar (approximately a mirror reflection) to the hardness profile for the AS 7075–RS 5083 configuration and the same rotational speed. For other speeds, the hardness in the stir zone decreased to 80 HV (base 5083 alloy hardness). This confirms that in this area of the stir zone, the 5083 alloy bands dominate. The fluctuations in hardness within the stir zone are associated with material mixing in this area. For both configurations, the maximum hardness in the stir zone was approximately 150 HV. This value remained constant from the weld center (point 0) up to approaching the 7075 alloy. It was observed that independent of the alloy configuration, on the 5083 alloy side, the hardness was about

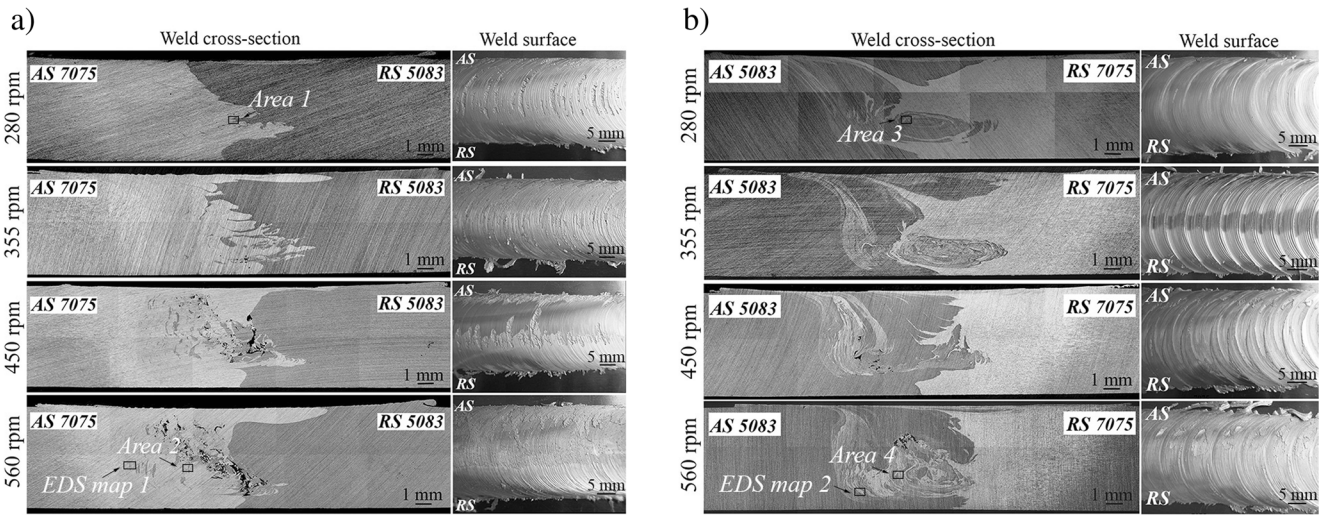

Fig. 4 Macrographic view of the cross-section and top surface of **a** AS 7075–RS 5083 welds and **b** AS 5083–RS 7075 welds (AS—advancing side, RS—retreating side), with marked areas of microstructural analysis; Triflute pin

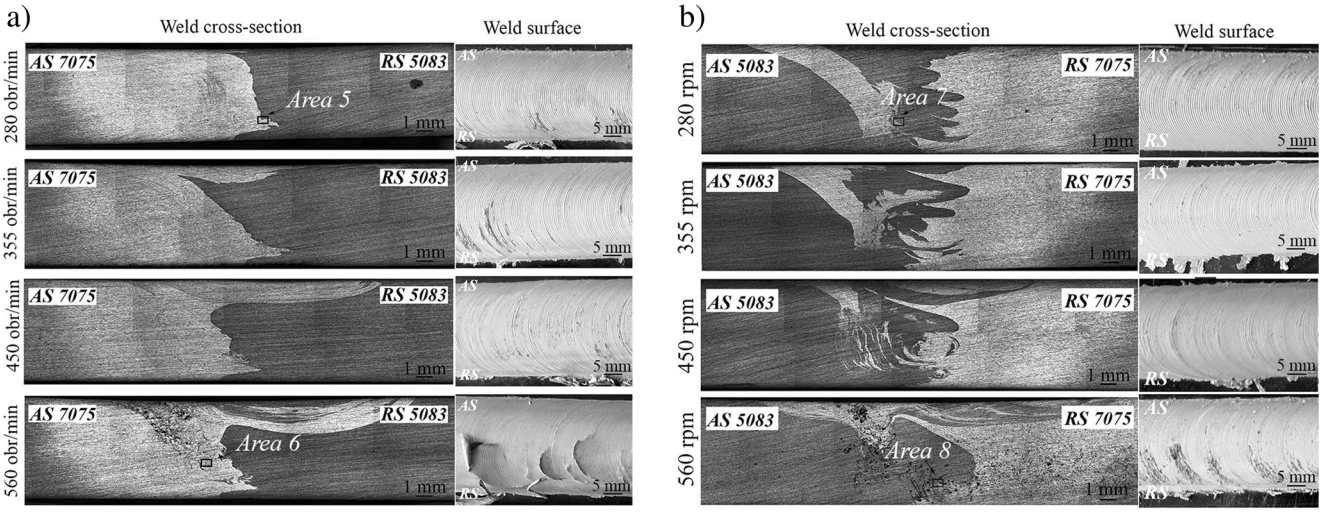

Fig. 5 Macrographic view of the cross-section and top surface of **a** AS 7075–RS 5083 welds and **b** AS 5083–RS 7075 welds, with marked areas of microstructural analysis; threaded taper pin

80 HV (base 5083 alloy hardness) and remained constant with increasing distance from the weld center. On the 7075 alloy side, the hardness decreased from 150 HV to 120 HV and then increased to 160 HV (at the distances up to 20 mm from weld center). The shape of hardness profile on the 7075 alloy side (half of a W-shape) is characteristic for most friction stir welds of heat-treatable alloys, welded in the peak aged or overaged conditions (T6/T7 tempers) [23].

Hardness profiles for welds produced with the threaded taper tool are displayed in Fig. 9. For particular alloy placements, the profiles were very similar to those found for the Triflute pin, but values of hardness were higher. The maximum hardness in the weld center even approached a value of 180 HV (for the AS 7075–RS 5083 joints fabricated at 280 and 450 rpm). For the AS 5083–RS 7075 configuration, the hardness in welds was about 160 HV. The small hardness fluctuations in this region are likely associated with the degree of material mixing (microstructural observation of alternately placed material bands).

A comparison of hardness profiles for welds produced with the Triflute pin and the threaded taper pin reveals the difference in hardness on the 7075 alloy side. For the Triflute pin, the hardness measured 20 mm away from the weld center on the 7075 side approached 160 HV. On the other hand, the hardness profiles for welds produced by the other pin, in the AS 7075–RS 5083 configuration, achieved a value of 180 HV at a distance of 15 mm. In the AS 5083–RS 7075 joints, the hardness was also 180 HV and also about 20 mm from the weld center. This observation confirms the macrostructural analysis. The stir zone area was narrow in the joints fabricated by the threaded taper tool.

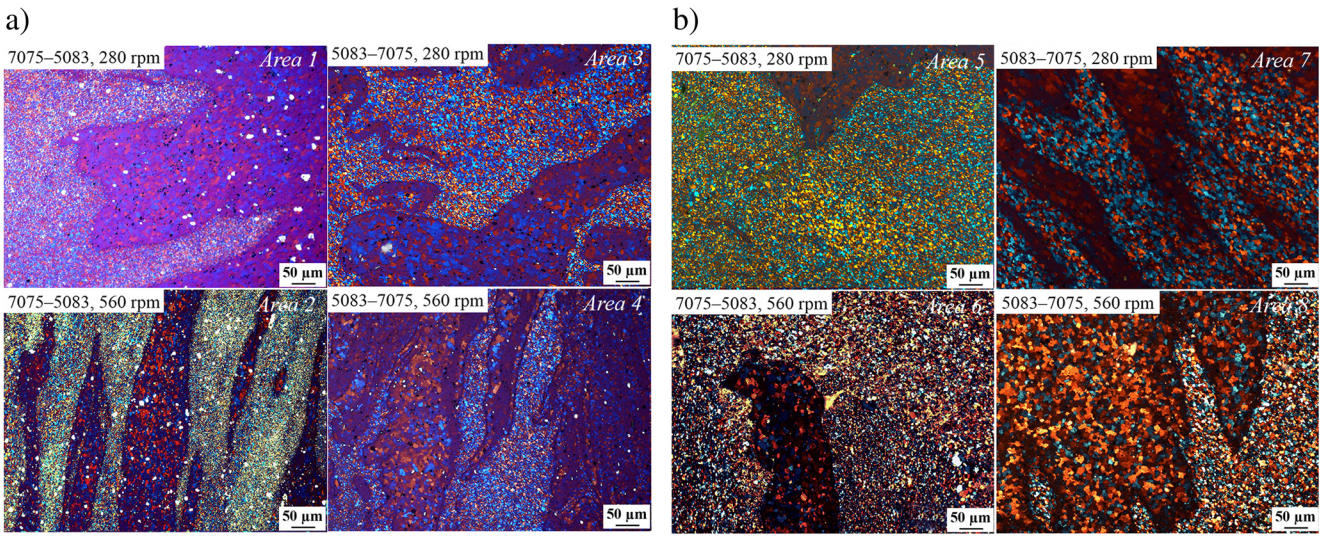

Fig. 6 Microstructure of the center region in welds produced at **a** Triflute pin and **b** threaded taper pin

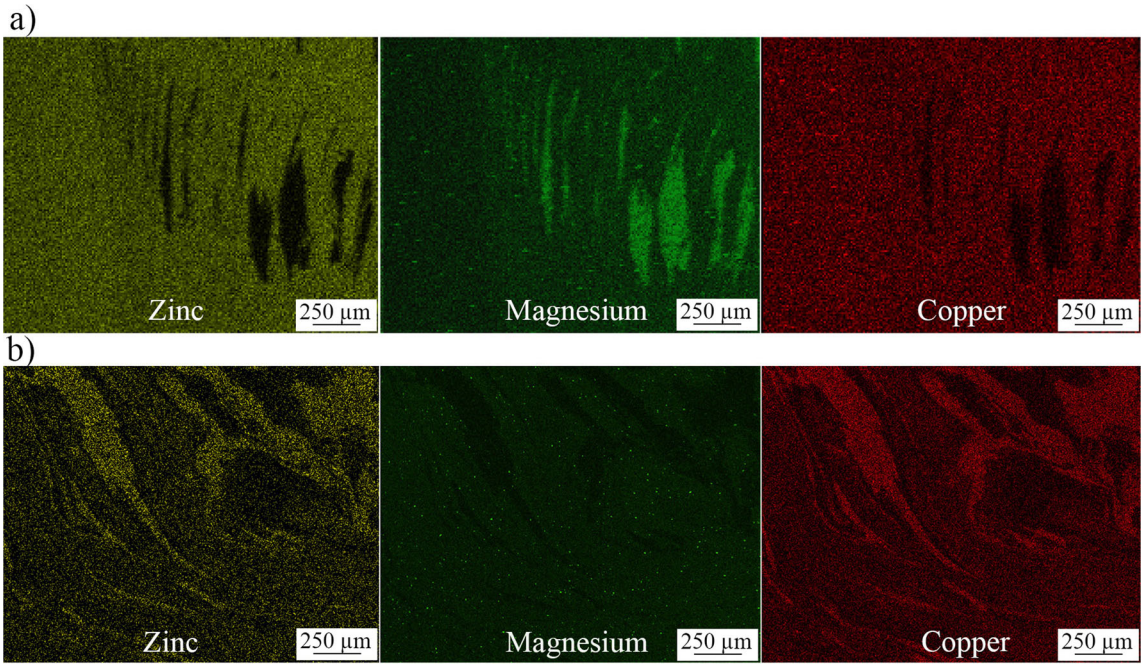

Fig. 7 Exemplary EDS maps of weld in configuration. **a** AS 7075–RS 5083. **b** AS 5083–RS 7075

It is important to note that in the case of the AS 7075–RS 5083 joints made with the threaded taper tool, on the 5083 alloy side, the hardness approaches a value higher than 80 HV, unlike the other tested welds.

3.4 Tensile tests

The results of tensile test for the welded specimens are listed in Tables 4 and 5, and representative stress–strain curves are provided in Fig. 10. The tensile test results for the joints fabricated with the Triflute pin (Table 4) show that the best mechanical properties are obtained for welds produced at 280 and 355 rpm speeds for both configurations. The maximum tensile strength and yield strength (371 and 308 MPa, respectively) are achievable for the AS 5083–RS 7075 weld produced at 280 rpm. The elongation of non-defective welds was above 9%. However, the elongation of these joints is lower than both the base alloys. The decrease in elongation is due to the clustering of the strengthening precipitates and also effect arising from the localization of strain occurring in the weld region during the FSW process [24]. These joints also indicated a large weld efficiency (i.e., the ratio of the tensile strength of the weld to the tensile strength of the softer welded alloy, in this case 5083 alloy), about 105%. Imperfections in the joint microstructure decrease mechanical properties. The welds produced at 450 rpm and especially 560 rpm were characterized by lower strength.

Table 5 presents the mechanical properties of welds fabricated with the threaded taper pin. As in the previously described joints, the highest strengths and weld efficiencies

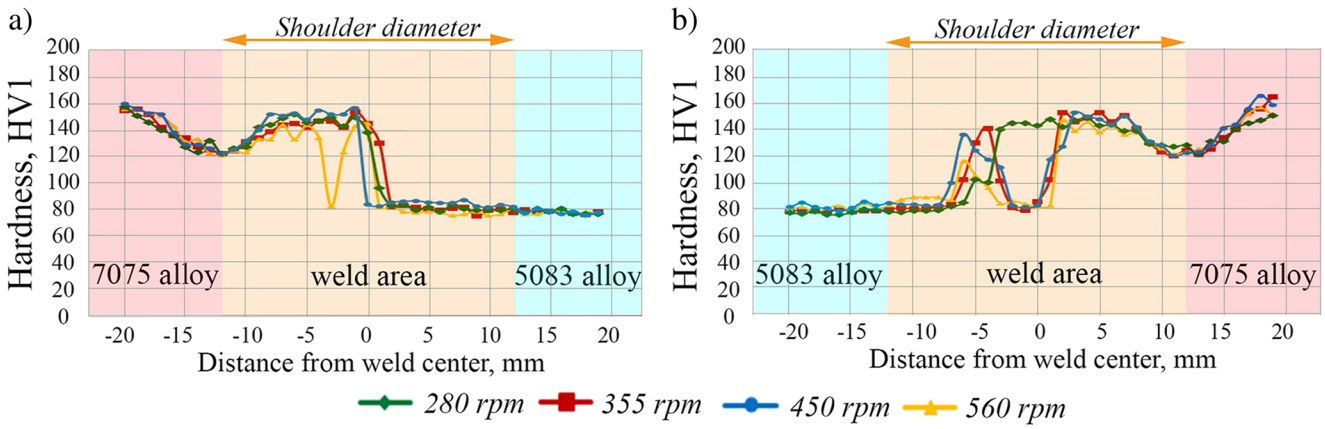

Fig. 8 Hardness profiles for **a** 7075–5083 weld and **b** 5083–7075 weld; 3 mm from weld surface, Triflute pin

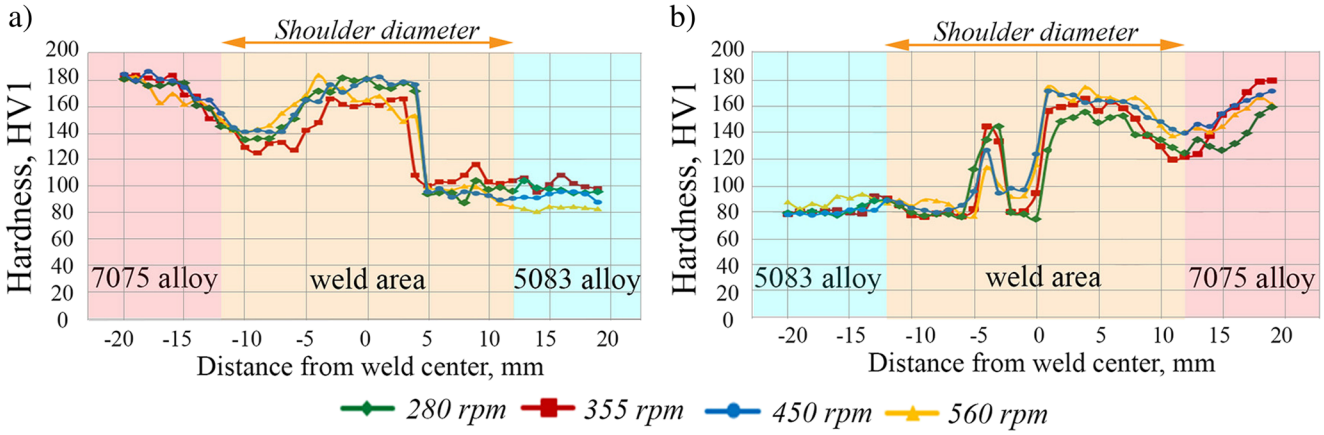

Fig. 9 Hardness profiles for **a** 7075–5083 weld and **b** 5083–7075 weld; 3 mm from weld surface, threaded taper pin

occurred at 280 and 355 rpm tool rotational speeds. However, the values of tensile stress and yield stress were approximately 22% lower, and the elongation was even 40% lower. The welds produced at 450 rpm exhibited a slightly lower tensile strength, especially for the AS 5083–RS 7075 configuration. The presence of macroscopic defects in joints performed at 560 rpm resulted in the fracture of tensile specimens in the elastic region.

Figure 11 shows photographs of samples after tensile testing. The rupture of samples produced at lower tool rotational speeds occurred at an angle of 45° in the base 5083 alloy. On the other hand, the AS 7075–RS 5083 joint produced at 355 rpm by the threaded taper pin fractured in the weld area near the retreating side. This may be related to the hardness decrease observed in the proximity of the fracture location. The fracture angle of 45° was also reported in other studies [16, 18]. In the case of welds fabricated at higher rotational speeds (450 and 560 rpm), fractures occurred in the weld area, exactly in the location of defects. This was confirmed by SEM observations of fracture surfaces (Figs. 12 and 13). However, fracture surfaces of tensile specimens for all defect-free tested joints displayed dominant ductile type of rupture (Fig. 12). Fracture surfaces were covered well-defined various dimple size.

4 Discussion

4.1 Effect of tool rotational speed

Tool rotational speed is one of the main parameters of the FSW process. This research shows that tool rotational speed influences the material mixing and the presence of defects as well. For both tools utilized, an increase in tool rotational speed results in better mixing of joined alloys due to the enhancement of plastic flow; however, numerous imperfections are simultaneously generated, and the quality of the top of the weld surface deteriorates. The defects are in the form of tunnel voids, wormholes, or porosity. These defects are especially formed when the rotational tool speeds are high, i.e., 450 rpm or 560 rpm for the Triflute tool or 560 rpm for the tapered threaded tool. For these parameters (with an increase in the tool rotational speed), the heat generation during the FSW process is relatively high. This leads to better material mixing on the one hand, but defect formation on the other. As reported by Mastanaiah [9], the increased heat input improves the contact between the material and the tool during welding. This helps in the formation of better metallurgical bonds. Therefore, the stronger the pin stirring action with the softer materials due to the higher temperature, the tendency to form

Table 4 Comparison of mechanical properties and weld efficiency for the obtained welds by Triflute tool (sample standard deviations in parentheses)

	Joint configuration							
	AS 7075–RS 5083				AS 5083–RS 7075			
	Tool rotational speed, rpm							
	280	355	450	560	280	355	450	560
Tensile strength, MPa	*364 (±0.7)*	*367 (± 0.0)*	336 (± 16.7)	204 (± 6.4)	*371 (± 3.1)*	*365 (± 0.8)*	354 (± 30.6)	292 (± 22.5)
0.2% yield strength, MPa	*302 (± 5.6)*	*302 (± 1.3)*	307 (± 1.3)	–	*308 (± 0.1)*	*305 (± 0.2)*	308 (± 4.2)	286 (± 25.6)
Elongation, %	9.4 (± 0.6)	9.9 (± 0.4)	4.0 (± 1.1)	0.5 (± 0.0)	9.9 (± 0.1)	9.1 (± 0.5)	6.1 (± 2.8)	2.5 (± 0.8)
Weld efficiency, %	105	106	97	59	107	105	102	84

Table 5 Comparison of mechanical properties and weld efficiency for the obtained welds by threaded taper tool (sample standard deviations in parentheses)

	Joint configuration							
	AS 7075–RS 5083				AS 5083–RS 7075			
	Tool rotational speed, rpm							
	280	355	450	560	280	355	450	560
Tensile strength, MPa	*287* (± *0.1*)	*286* (± *6.1*)	238 (± 0.3)	157 (± 40.0)	*282* (± *0.1*)	*286* (± *1.5*)	280 (± 3.9)	111 (± 75.3)
0.2% yield strength, MPa	*236* (± *3.0*)	*236* (± *2.3*)	228 (± 2.7)	–	*236* (± *1.0*)	*242* (± *3.5*)	234 (± 5.6)	–
Elongation, %	6.2 (± 0.4)	7.1 (± 1.8)	4.5 (± 0.2)	2.0 (± 0.6)	6.7 (± 0.2)	5.8 (± 2.6)	6.1 (± 0.1)	1.7 (± 0.8)
Weld efficiency, %	83	83	69	45	82	83	81	32

defects is smaller. This in turn leads to stronger intermixing of alloys. Saedi et al. [18] reported similar observations that occurred upon the decrease of the traverse speed. The most defective AS 5083–RS 7075 joints were welded at low traverse speed. A decrease in the traverse speed generated more heat resulting in the creation of tunnel-type defects.

It is important to note that the grain size does not change with an increase in the tool rotational speed. An increase of rotational speed, at a constant traverse speed, generates more heat. According to Saedi et al. [18] and Ghosh [11], the reduction in the heat input and the rise of strain with increasing traverse speed, at a constant tool rotational speed, lead to a decrease of the grain size. Also, Ugender et al. [25] reported that a higher rotational speed produces more heat per unit length and contributes to a slower cooling rate in the particular FSW zones. This, in turn, gives rise to grain growth. However, in this study, for the applied parameters, the heat generated is insufficient for coarsening the grains, or precipitates limit grain growth.

Obviously, the macroscopic defects as well as degree of material stirring in dissimilar joints determine the mechanical properties. In this research, the influence of the tool rotational speed on hardness profiles was negligible. Regardless of the tool rotational speed, the hardness of the tested welds was similar. However, the higher tool rotational speed at a constant traverse speed leads to a decrease in the tensile strength. This decrease is also attributed to the presence of defects that begin to form at higher rotational speeds in the stir zone. However, based on the literature, a trend in the relationship between tensile strength and tool rotational speed is ambiguous. For example, Saedi et al. [18] observed that with an increase in tool rotational speed from 450 to 800 rpm, at a selected traverse speed (30, 41.5, or 50 mm/min), the tensile strength initially decreased and then increased. Palanivel et al. [6]

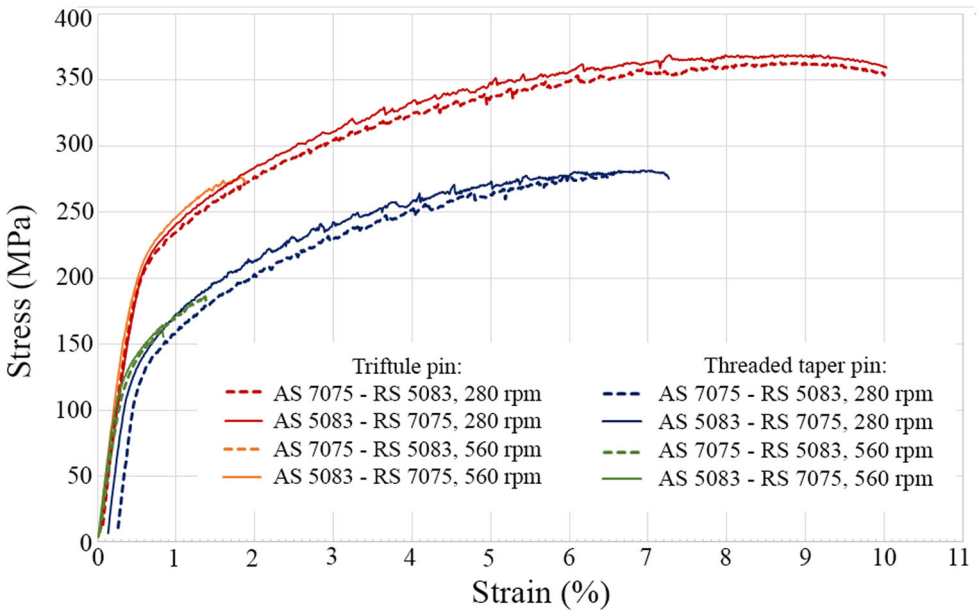

Fig. 10 Representative stress–strain curves for the selected welds

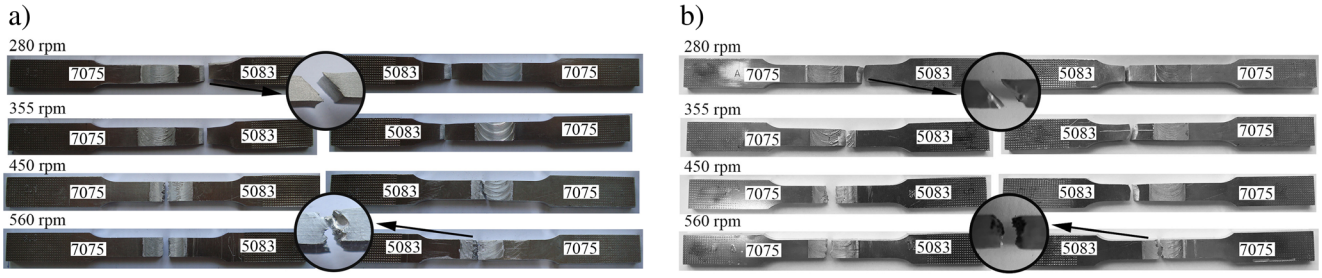

Fig. 11 Location of fracture in tensile specimens. **a** Triflute pin. **b** Threaded taper pin

noticed an opposite relationship: with an increasing tool rotational speed (from 600 to 1300 rpm) at a constant traverse speed of 60 mm/s, for different pin geometry, the tensile strength initially increased and then decreased. Also, Sivachidambaram et al. [8] presented three various relations for different traverse speeds (40, 60, and 80 mm/min). This demonstrates that the effect of tool rotational speed on mechanical properties is not clear because it is strongly dependent on other parameters, e.g., traverse speed and the type of materials joined.

4.2 Effect of pin design

During the friction stir welding process, the type of pin profile directly affects material flow, heat generation, and shearing action of plasticized materials [3, 22]. This investigation shows that the tool geometry has a clear influence on the degree of intermixing of alloys joined and the extent of the weld area. The joints produced with the Triflute pin display better material mixing producing a more complex microstructure in the stir zone with finer recrystallized grains than welds produced using the threaded taper pin. Because the shape of Triflute pin is cylindrical (not narrowed at the end as taper pin), the region of the stirred zone is wider and more square on the weld cross-sections. However, in the case of the Triflute pin, microdefects occur near the stir zone at 355 and 450 rpm tool rotational speeds for the AS 7075–RS 5083 and AS 5083–RS 7075 configurations, respectively. For the taper pin, the flaws are observed at 560 rpm. This suggests that Triflute pin gives rise to a larger heat input, a finding previously suggested by Thomas et al. [26].

The pin design is responsible for material intermixing and thereby for final mechanical properties. In spite of the similar trend in the relationship between mechanical properties/tool rotational speed for both tools, the Triflute pin improves the strength and joint efficiency. The tensile strength was about 80 MPa higher than for the taper pin. For the defect-free welds, the joint efficiency even approached 107%. In other published studies on dissimilar welds of 5083 and 7075 alloys, the weld efficiency was lower, i.e., 77–87% [19], 87% [17], and approximately 84% [18].

The maximum hardness achieved in the stir zone also depended on the FSW tool utilized. The welds fabricated by the Triflute pin were characterized by a maximum hardness of

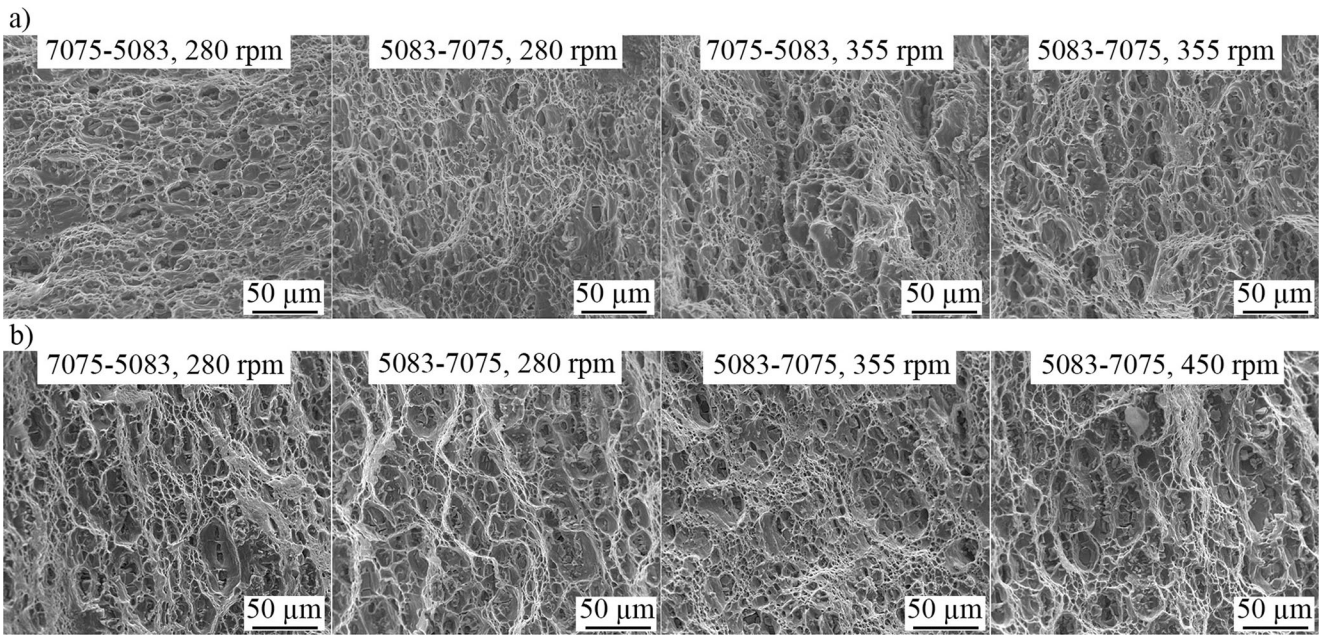

Fig. 12 The SEM microphotographs of fracture surface of tensile specimens for defect-free welds. **a** Triflute pin. **b** Threaded taper pin

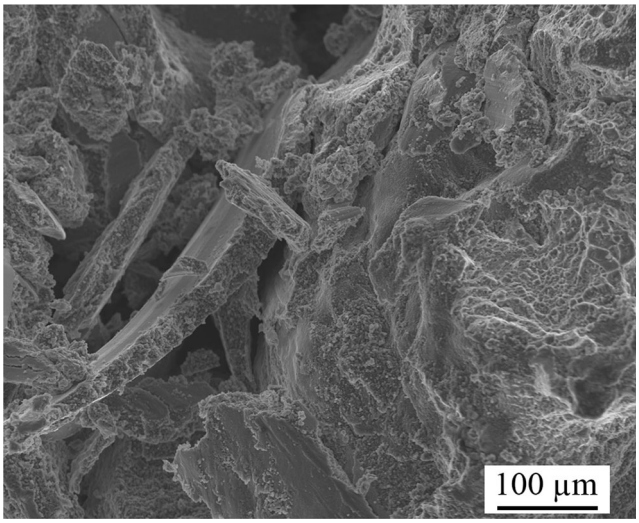

Fig. 13 Exemplary SEM microphotograph of fracture surface of defective weld specimen

150 HV, whereas in the case of the threaded taper pin, the highest hardness in the stir zone was 180 HV (for the AS 7075–RS 5083 configuration) and 160 HV (for the AS 5083–RS 7075 configuration). It is worth noting that, as mentioned earlier, for the Triflute pin, a smaller grain size was observed than in the case of second tool. Bahemmat et al. [27], likewise, noticed that for the dissimilar 7075-O and 2024-T4 joints, the average hardness value in the four-flute tool case was lower, and microstructural analysis also showed that the grain size was smaller than in the threaded taper pin case. However, the researchers suggested that the grain size was not a dominating factor influencing microhardness in these welds. The dependence of grain size upon the pin profile was also observed by Aval [13]. However, in Aval's work, the relationship between grain size and hardness was not clear.

4.3 Effect of alloy configuration

The configuration of welded alloys is a very important factor in FSW joining of dissimilar materials [1, 12]. Since recent publications do not give definitive direction as to the optimal weld configuration (i.e., the placement of the alloy on the retreating or advancing side), the examined joints were produced in two configurations. Some researchers [10, 14, 28, 29] reported that when the weaker alloy is placed on the retreating side, the produced weld becomes weaker compared to the opposite configuration. However, according to other investigations [12, 13, 30], the more efficient mixing of materials and better properties can be achieved with the softer alloy on the advancing side and the harder alloy on the retreating side.

This study clearly shows that the placement of base materials exerts a distinct effect on the material mixing. Regardless of pin profile, for the welds performed in the AS 5083–RS 7075 configuration, the intensive material intermixing and lesser amount of defects for higher tool rotational speeds were observed. In the case of the opposite configuration, the joined alloys were stirred only at higher tool rotational speeds, but it brought about the generation of numerous defects. The alloy configuration affected the content of the main constituent elements, which came from base materials, in the stir zone. The EDS analysis revealed that the dominant elements in the stir zone came from the alloy located on the advancing side while the observed bands differed in the content of zinc, magnesium, and copper.

A significant influence of alloy location on mechanical behavior and hardness was not found. The placement of alloys did not impact on maximum hardness value in stirred zone in welds produced by Triflute tool. However, for the welds produced by the threaded taper tool, a difference in maximum hardness in stir zone was observed. For the AS 7075–RS 5083 joints, the highest hardness was even 180 HV and for the opposite weld configuration was about 160 HV. Depending on alloy location, the zone with the highest hardness was near the advancing side and in the weld center (for 7075–5083 welds) or near retreating side (for 5083–7075 welds). For applied FSW parameters, the weld configuration did not effect on mechanical properties. The final mechanical properties of welds are dependent on not only degree of material mixing (concentration of alloying), but also grain size or strengthening precipitates.

5 Conclusions

The research showed that 7075 and 5083 aluminum alloys can be successfully joined by FSW if the process parameters are appropriately selected. The detailed conclusions are as follows:

1. The defect-free joint with the highest mechanical properties was fabricated with 5083 on the advancing side and 7075 on the retreating side, using the Triflute pin and a tool rotational speed of 280 rpm.
2. The formation of the stir zone was dependent on tool rotational speed and the direction of stirring, i.e., on the alloy placement during welding. Better mixing of materials was obtained at higher rotational speeds and for the AS 5083–RS 7075 weld configuration; however, under these conditions, more defects were found in the weld microstructure.
3. The pin geometry influenced the shape of the stir zone. A wider area of this zone was obtained for welds fabricated by the Triflute pin.
4. Regardless of the tool, the pin type, or the weld configuration, the mechanical properties and joint efficiency decreased with an increase in the tool rotational speed;

however, this was associated with an increase in the number of defects.
5. The enhancement of tensile strength and weld efficiency (above 100%) was obtained with utilization of the Triflute pin.
6. The effect of alloy placement during welding on mechanical properties was negligible.
7. The defect-free tensile specimens fractured within the 5083 alloy (softer base material).

Funding information The research project was financed by the Polish National Science Centre (No: DEC-2012/07/D/ST8/02737).

References

1. DebRoy T, Bhadeshia HKDH (2010) Friction stir welding of dissimilar alloys—a perspective. Sci Technol Weld Join 5:266–270. https://doi.org/10.1179/174329310X12726496072400
2. Murr LE (2010) A review of FSW research on dissimilar metal and alloy systems. J Mater Eng Perform 19:1071–1089. https://doi.org/10.1007/s11665-010-9598-0
3. Mishra RS, Mahoney MW (2007) Friction stir welding and processing. ASM International, Ohio
4. Babu AS, Devanathan C (2013) An overview of friction stir welding. Int J Res Mech Eng Technol 3:259–265
5. Pandya SN, Menghani JV (2013) Friction stir welding of dissimilar 5xxx to 6xxx Al alloys: a review. Appl Mech Mater 376:42–48. https://doi.org/10.4028/www.scientific.net/AMM.376.42
6. Palanivel R, Koshy Mathews P, Murugan N, Dinaharan I (2012) Effect of tool rotational speed and pin profile on microstructure and tensile strength of dissimilar friction stir welded AA5083-H111 and AA6351-T6 aluminum alloys. Mater Des 40:7–16. https://doi.org/10.1016/j.matdes.2012.03.027
7. Kasman S, Yenier Z (2014) Analyzing dissimilar friction stir welding of AA5754/AA7075. Int J Adv Manuf Technol 70:145–156
8. Sivachidambaram S, Rajamurugan G, Amirtharaj D (2015) Optimizing the parameters for friction stir welding of dissimilar aluminium alloys AA5383/AA7075. ARPN J Eng Appl Sci 10:5434–5437
9. Mastanaiah P, Sharma A, Reddy GM (2016) Dissimilar friction stir welds in AA2219-AA5083 aluminum alloys: effect on process parameters on material inter-mixing, defect formation and mechanical properties. Trans Indian Inst Metals 69:1397–1415. https://doi.org/10.1007/s12666-015-0694-6
10. Cavaliere P, De Santis A, Panella F, Squillace A (2009) Effect of welding parameters on mechanical and microstructural properties of dissimilar AA6082-AA2024 joints produced by friction stir welding. Mater Des 30:609–616. https://doi.org/10.1016/j.matdes.2008.05.044
11. Ghosh M, Husain MM, Kumar K, Kailas SV (2013) Friction stir-welded dissimilar aluminum alloys: microstructure, mechanical properties, and physical state. J Mater Eng Perform 22:3890–3901. https://doi.org/10.1007/s11665-013-0663-3
12. Guo JF, Chen HC, Sun CN, Bi G, Sun Z, Wei J (2014) Friction stir welding of dissimilar materials between AA6061 and AA7075 Al alloys effects of process parameters. Mater Des 56:185–192. https://doi.org/10.1016/j.matdes.2013.10.082
13. Aval HJ (2015) Influences of pin profile on the mechanical and microstructural behaviors in dissimilar friction stir welded AA6082–AA7075 butt joint. Mater Des 67:413–421. https://doi.org/10.1016/j.matdes.2014.11.055
14. Reza-E-Rabby M, Tang W, Reynolds AP (2015) Effect of tool pin features on process response variables during friction stir welding of dissimilar aluminum alloys. Sci Technol Weld Join 20:425–432. https://doi.org/10.1179/1362171815Y.0000000036
15. Ilangovan M, Boopathy SR, Balasubramanian V (2015) Effect of tool pin profile on microstructure and tensile properties of friction stir welded dissimilar AA 6061–AA 5086 aluminium alloy joints. Def Technol 11:174–184. https://doi.org/10.1016/j.dt.2015.01.004
16. Shojaeefard MH, Behnagh RA, Akbari M, Givi MKB, Farhani F (2013) Modelling and Pareto optimization of mechanical properties of friction stir welded AA7075/AA5083 butt joints using neural network and particle swarm algorithm. Mater Des 44:190–198. https://doi.org/10.1016/j.matdes.2012.07.025
17. Ahmed AZ, Abbass MK, Ataiwi AH, Khanna SK, Jashti B, Widener C (2014) Investigation of fatigue behavior and fractography of dissimilar friction stir welded joints of aluminum alloys 7075-T6 and 5052-H34. Int J Mater Sci Eng 2:115–121. https://doi.org/10.12720/ijmse.2.2.115-121
18. Saeidi M, Manafi B, Givi MKB, Faraji G (2015) Mathematical modeling and optimization of friction stir welding process parameters in AA5083 and AA7075 aluminum alloy joints. Proc Inst Mech Eng B J Eng 1:1–11. https://doi.org/10.1177/0954405415573697
19. Ahmed MMZ, Ataya S, El-Sayed Seleman MM, Ammar HR, Ahmed E (2017) Friction stir welding of similar and dissimilar AA7075 and AA5083. J Mater Process Technol 24:277–291. https://doi.org/10.1016/j.jmatprotec.2016.11.024
20. Chen Y, Ding H, Cai Z, Zhao J, Li J (2017) Microstructural and mechanical characterization of a dissimilar friction stir-welded AA5083-AA7B04 butt joint. J Mater Eng Perform 26:530–539. https://doi.org/10.1007/s11665-016-2482-9
21. Kalemba-Rec I, Hamilton C, Kopyściański M, Miara D, Krasnowski K (2017) Microstructure and mechanical properties of friction stir welded 5083 and 7075 aluminum alloys. J Mater Eng Perform 26:1032–1043. https://doi.org/10.1007/s11665-017-2543-8
22. Nandan R, DebRoy T, Bhadeshia HKDH (2008) Recent advances in friction-stir welding—process, weldment structure and properties. Prog Mater Sci 53:980–1023. https://doi.org/10.1016/j.pmatsci.2008.05.001
23. Threadgill PL, Leonard AJ, Shercliff HR, Withers PJ (2009) Friction stir welding of aluminum alloys. Int Mater Rev 54:49–93. https://doi.org/10.1179/174328009X411136
24. Shanmuga SN, Murugan N (2010) Tensile behavior of dissimilar friction stir welded joints of aluminium alloys. Mater Des 31:4184–4193. https://doi.org/10.1016/j.matdes.2010.04.035
25. Ugender S, Kumar A, Reddy AS (2014) Experimental investigation of tool geometry on mechanical properties of friction stir welding of AA 2014 aluminium alloy. Procedia Mater Sci 5:824–831. https://doi.org/10.1016/j.mspro.2014.07.334

26. Thomas WM, Johnson KI, Wiesner CS (2003) Friction stir welding—recent developments in tool and process technologies. Adv Eng Mater 5:485–490
27. Bahemmat P, Haghpanahi M, Givi MKB, Seighalani KR (2012) Study on dissimilar friction stir butt welding of AA7075-O and AA2024-T4 considering the manufacturing limitation. Int J Adv Manuf Technol 59:939–953. https://doi.org/10.1007/s00170-011-3547-4
28. Bahemmat P, Haghpanahi M, Besharati MK, Ahsanizadeh S, Rezaei H (2010) Study on mechanical, micro and macrostructural characteristics of dissimilar friction stir welding of AA6061-T6 and AA7075-T6. Proc Inst Mech Eng B J Eng 224:1854–1864. https://doi.org/10.1243/09544054JEM1959
29. Kishore VR, Arun J, Padmanabhan R, Balbasubramanian V (2015) Parametric studies of dissimilar friction stir welding using computational fluid dynamics simulation. Int J Adv Manuf Technol 80:91–98. https://doi.org/10.1007/s00170-015-6995-4
30. Park SK, Hong ST, Park JH, Park KY, Kwon YJ, Son HJ (2010) Effect of material locations on properties of friction stir welding joints of dissimilar aluminium alloys. Sci Technol Weld Join 15:331–336. https://doi.org/10.1179/136217110X12714217309696